inter.noise
HAMBURG 2016

Application of Nonlinear Adaptive Filter to Narrowband Active Noise Control in the Presence of Frequency Mismatch

Jian LIU[1]; Yegui XIAO[2]

[1] Nanjing University of Aeronautics and Astronautics, Nanjing, China
[2] Prefectural University of Hiroshima, Hiroshima, Japan

ABSTRACT

To avoid acoustic feedback, a non-acoustic sensor such as tachometer or accelerometer is usually employed to identify synchronization frequency in a narrowband active noise control (ANC) system which has been widely and effectively applied in mitigating periodic or nearly periodic noises generated by rotating machines. Frequency mismatch (FM), i.e. the difference between identified synchronization frequency and true frequency of primary noise, may exist for the sensor aging effects, fatigue accumulation, etc. A conventional narrowband ANC system will suffer severe performance degradation even for an FM as small as 1% and several structures have been developed for removing FM. This work presents a new narrowband ANC structure coupled with a nonlinear adaptive filter for mitigating FM. The nonlinear adaptive filters such as popular Volterra filter and functional link artificial neural network (FLANN) or their modifiers are considered. Simulations are conducted to demonstrate the effectiveness of the designed new nonlinear narrowband ANC system on coping with FM problem.

Keywords: Narrowband active noise control (NANC), Frequency mismatch (FM), Nonlinear filter, Filtered-X LMS (FXLMS)
I-INCE Classification of Subjects Number(s): 74.9

1. INTRODUCTION

Narrowband active noise control (NANC) system has been widely and effectively used for suppressing sinusoidal noise generated by rotating machines and devices with reciprocating motion (1, 2, 3, 4). To avoid acoustic feedback from the cancelling loudspeaker to the reference microphone, a non-acoustic sensor such as tachometer is usually employed to identify synchronization frequency in a NANC system (3, 5). The filtered-X LMS (FXLMS) algorithm (6, 7) is a classical ANC adaptive algorithm and most commonly used to update weights of the control filter. It has been proved that, in some real-life applications, a linear NANC system may suffer from performance degradation due to the presence of even less than 1% frequency mismatch (FM) which is essentially the difference between reference signal frequency and primary noise signal frequency and occurs because of the sensor aging effects, fatigue accumulation, time-varying primary noise source, etc (8). So far, many works have focused on analytically investigating the FM effects, and several modified algorithms have been proposed to mitigate the FM in a considerable degree (9, 10, 11, 12, 13, 14, 15, 16, 17). It should be noted that, in (8), an auto recursive (AR) model which is essentially a second order adaptive finite-impulse response (FIR) notch filter was designed for accommodating FM. In fact, this second order AR model is a relatively simple and effective way for mitigating small FM, and presents promising performance in applications at the same time, which has been verified in later works, such as (11, 12, 16).

On the other hand, to handle nonlinear distortion problem, many nonlinear structures, such as network based algorithms (18, 19, 20, 21) especially functional link artificial neural network (FLANN) (22, 23, 24, 25, 26, 27) and Volterra filter (28, 29, 30, 31), were developed and proposed for ANC. In fact, the presence of FM may be regarded as one kind of nonlinearity. With this in mind, this paper tries to develop new FM accommodating approaches with nonlinear filter and AR model. In detail, nonlinear filters including Volterra filter, FLANN, and recursive FLANN are investigated. In the new systems, the typical FXLMS algorithm is still adopted.

The remainder of this paper is organized as follows. The general FXLMS-based nonlinear NANC system with AR model is given in Section 2. In this Section, the Volterra filter, FLANN, recursive FLANN, cor-

[1] jliu@nuaa.edu.cn
[2] xiao@pu-hiroshima.ac.jp

responding expressions and FXLMS-based weights updating difference equations are also derived in brief. Representative simulation results will be provided in Section 3 to confirm the effectiveness of the proposed system. Section 4 concludes the paper.

2. FXLMS-BASED NONLINEAR NANC SYSTEM WITH AR MODEL

2.1 general diagram block

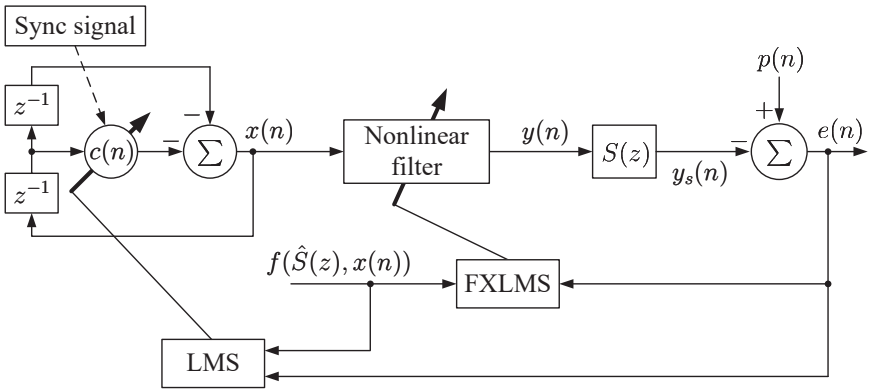

Figure 1 – General diagram block of FXLMS-based nonlinear NANC system with AR model (single tone).

From (8), in a similar way, it is very easy to design a general diagram block of FXLMS-based nonlinear NANC system with AR model as shown in Figure 1. The primary sinusoidal noise signal shown in Figure 1 is given by

$$p(n) = a_p \cos(\omega_p n) + b_p \sin(\omega_p n) + v_p(n), \tag{1}$$

where ω_p is the frequency of the primary sinusoidal noise, $\{a_p, b_p\}$ are corresponding discrete Fourier coefficients (DFCs), and $v_p(n)$ is a zero-mean additive white Gaussian noise with variance σ_p^2. The reference signal $x(n)$ generated based on a AR model and synchronization (sync) signal is denoted as

$$\begin{aligned} &x(n) = -c(n)x(n-1) - x(n-2), \quad (n \geq 2), \\ &c(0) = c(1) = -2\cos(\omega), \\ &x(0) = a, \quad x(1) = a\cos(\omega) + b\sin(\omega), \end{aligned} \tag{2}$$

where ω is the frequency of the reference signal which is obtained by means of a linear relationship between the sync signal, e.g., rotational speed obtained by non-acoustic sensor, and the signal fundamental frequency. Coefficients a and b can be usually set to 1.0. Now, the FM can be defined as

$$\Delta\omega = \omega_p - \omega, \tag{3}$$

which denotes the difference between reference signal frequency and the real primary noise frequency.

It is easy to see from Figure 1 that the residual noise signal of the system is calculated by

$$\begin{aligned} e(n) &= p(n) - y_s(n) \\ &= p(n) - \sum_{j=0}^{M-1} s_j y(n-j), \end{aligned} \tag{4}$$

where the output of the nonlinear filter, $y(n)$, is the secondary source. In equation (4), coefficients $\{s_j\}_{j=0}^{M-1}$ are impulse response series of the secondary path $S(z)$ with order $M-1$. The FIR-type $S(z)$ and its estimation model $\hat{S}(z)$ with coefficients $\{\hat{s}_m\}_{m=0}^{\hat{M}-1}$ and order $\hat{M}-1$ may be given as following expressions:

$$S(z) = \sum_{j=0}^{M-1} s_j z^{-j}, \quad \hat{S}(z) = \sum_{m=0}^{\hat{M}-1} \hat{s}_m z^{-m}. \tag{5}$$

The FXLMS and LMS algorithms respectively for nonlinear control filter weights and AR model coefficient $c(n)$ strictly depend on $f(\hat{S}(z), x(n))$ which is determined by nonlinear filter type and it is a nonlinear function with respect to the reference signal $x(n)$ and the secondary path estimate $\hat{S}(z)$.

2.2 using Volterra filter

A causal Volterra filter with a finite memory of L_V and a finite order of P can be described by following relationships (32):

$$y(n) = \sum_{p=1}^{P} y_p(n), \tag{6}$$

$$y_p(n) = \sum_{m_1=0}^{L_V-1} \sum_{m_2=m_1}^{L_V-1} \cdots \sum_{m_p=m_{p-1}}^{L_V-1} h_{p,m_1,m_2,\ldots,m_p}(n)x(n-m_1)x(n-m_2)\cdots x(n-m_p), \tag{7}$$

where $x(n)$ and $y(n)$ are respectively input and output of the Volterra filter and $h_{p,m_1,m_2,\cdots,m_p}(n)$ is the pth-order weight corresponding to Volterra kernel with the same order. Figure 2 shows a typical adaptive Volterra filter with both memory and order of 2. In real-life applications, memory and order of the filter usually should be set to be larger.

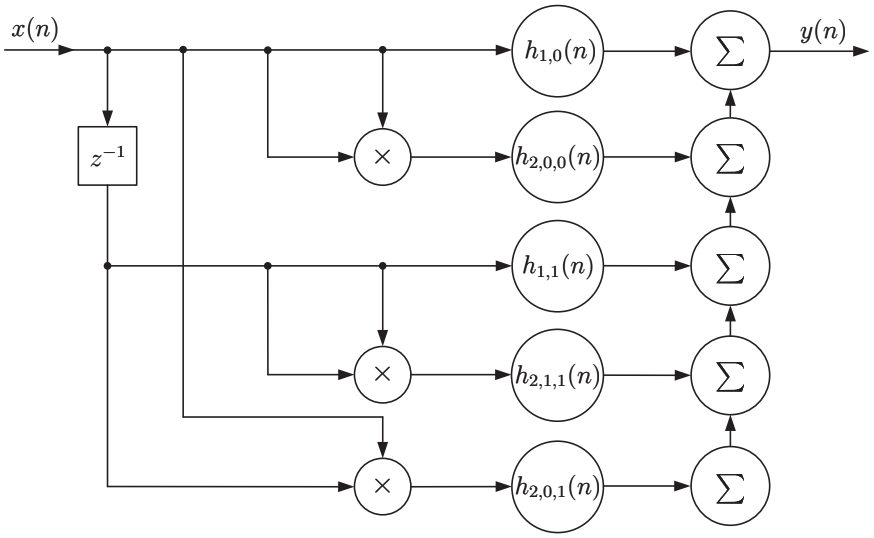

Figure 2 – A Volterra filter with both memory and order of 2.

When using a Volterra filter to the system depicted in Figure 1 as a control filter, the secondary source produced by the filter, $y(n)$, can be written as

$$\begin{aligned} y(n) = & \sum_{i=0}^{L_V-1} h_{1,i}(n)x(n-i) \\ & + \sum_{i=0}^{L_V-1} \sum_{j=i}^{L_V-1} h_{2,i,j}(n)x(n-i)x(n-j) \\ & + \sum_{i=0}^{L_V-1} \sum_{j=i}^{L_V-1} \sum_{k=j}^{L_V-1} h_{3,i,j,k}(n)x(n-i)x(n-j)x(n-k) \\ & + \cdots . \end{aligned} \tag{8}$$

Now, it is very easy to derive FXLMS algorithm for updating weights $h_{p,m_1,m_2,\cdots,m_p}(n)$ as (only difference equations for 1 to 3 orders are given)

$$h_{1,i}(n+1) = h_{1,i}(n) + \mu_1 e(n)\hat{x}(n), \tag{9}$$

$$h_{2,i,j}(n+1) = h_{2,i,j}(n) + \mu_2 e(n)\hat{x}(n-i)\hat{x}(n-j), \tag{10}$$

$$h_{3,i,j,k}(n+1) = h_{3,i,j,k}(n) + \mu_3 e(n)\hat{x}(n-i)\hat{x}(n-j)\hat{x}(n-k), \tag{11}$$

$$i = 0,1,\ldots,L_V-1; j = i,i+1,\ldots,L_V-1; k = j,j+1,\ldots,L_V-1.$$

Where, μ_1, μ_2, and μ_3 are step sizes. Filtered-X reference signal $\hat{x}(n)$ is obtained through feeding reference signal $x(n)$ to the secondary path estimate $\hat{S}(z)$, and it can be calculated as

$$\hat{x}(n) = \sum_{m=0}^{\hat{M}-1} \hat{s}_m x(n-m). \tag{12}$$

In addition, it is also not difficult to derive LMS algorithm for updating AR model coefficient $c(n)$ as

$$c(n+1) = c(n) - \mu_c e(n)\hat{x}_s(n), \tag{13}$$
$$\hat{x}_s(n) = h_{1,0}(n)\hat{x}(n-1) + 2h_{2,0,0}(n)\hat{x}(n)\hat{x}(n-1) + 3h_{3,0,0,0}(n)\hat{x}^2(n)\hat{x}(n-1) + \cdots,$$

where μ_c is the step size.

2.3 using FLANN with trigonometric functional expansions

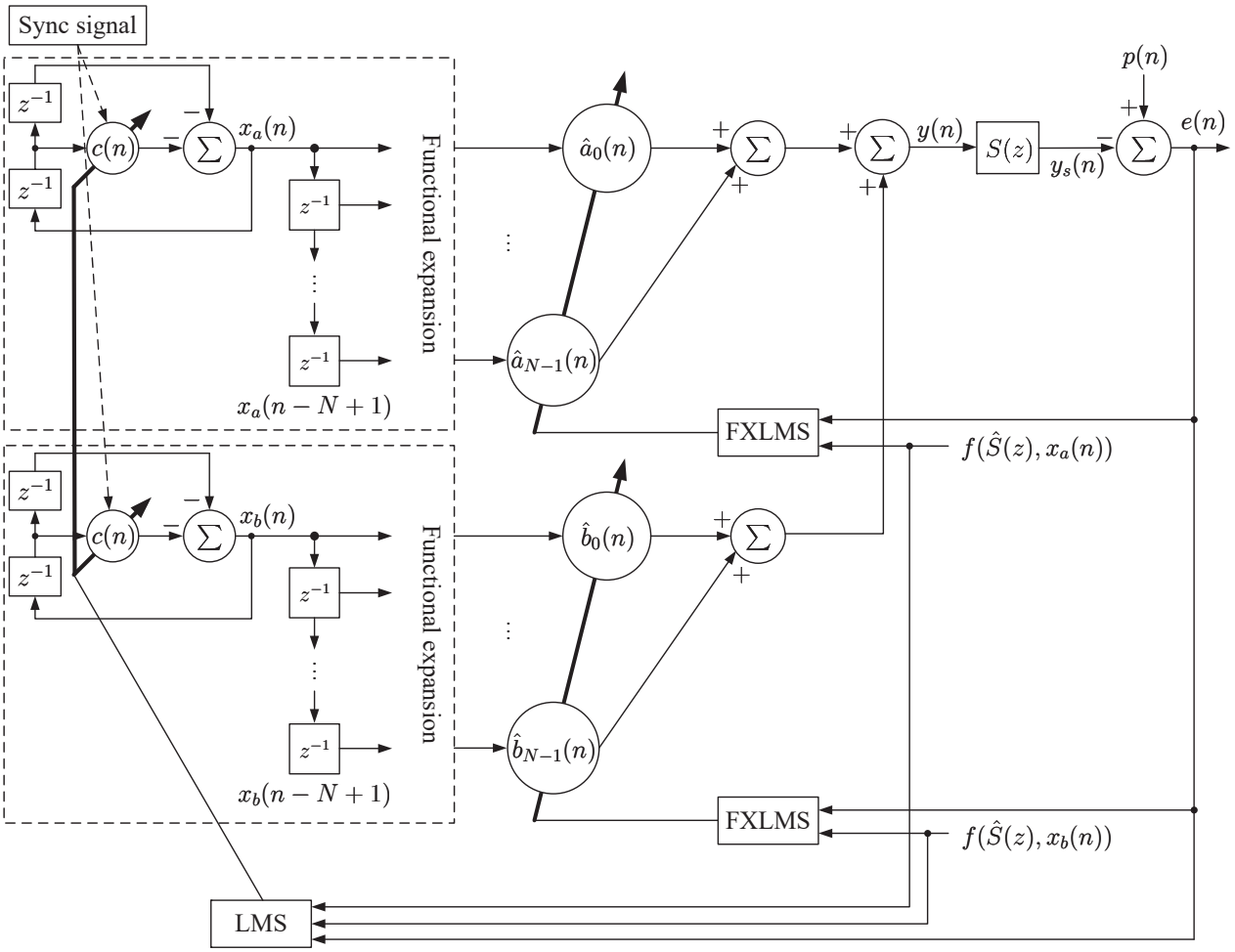

Figure 3 – Diagram block of nonlinear NANC system with FLANN and AR model (single tone).

FLANN with trigonometric functional expansions are used most popularly in ANC (23, 25, 26, 27) and Figure 3 gives a typical corresponding NANC system with FLANN and AR model for accommodating FM. In Figure 3, $x_a(n)$ and $x_b(n)$ are sinusoidal reference signals calculated by

$$x_a(n) = -c(n)x_a(n-1) - x_a(n-2), \quad (n \geq 2) \tag{14}$$
$$x_b(n) = -c(n)x_b(n-1) - x_b(n-2), \quad (n \geq 2) \tag{15}$$
$$c(0) = c(1) = -2\cos(\omega),$$
$$x_a(0) = a, \quad x_a(1) = a\cos(\omega),$$
$$x_b(0) = b, \quad x_b(1) = b\sin(\omega).$$

As indicated in Figure 3, if functional expansions are simply set to be trigonometric, the secondary source $y(n)$ can be finally expressed as

$$y(n) = \boldsymbol{w}_a^T(n)\boldsymbol{x}_a(n) + \boldsymbol{w}_b^T(n)\boldsymbol{x}_b(n), \tag{16}$$

where

$$\boldsymbol{w}_a(n) = [\hat{a}_0(n), \hat{a}_1(n), \ldots, \hat{a}_{N-1}(n)]^T, \tag{17}$$

$$\boldsymbol{w}_b(n) = [\hat{b}_0(n), \hat{b}_1(n), \ldots, \hat{b}_{N-1}(n)]^T, \tag{18}$$
$$\boldsymbol{x}_a(n) = [x_a(n), x_a(n-1), \ldots, x_a(n-N+1)]^T, \tag{19}$$
$$\boldsymbol{x}_b(n) = [x_b(n), x_b(n-1), \ldots, x_b(n-N+1)]^T. \tag{20}$$

Applying the steepest descent method, we can easily derive the FXLMS and LMS algorithms for updating control filter weights and AR model coefficient respectively as

$$\hat{a}_k(n+1) = \hat{a}_k(n) + \mu e(n)\hat{x}_a(n-k), \tag{21}$$
$$\hat{b}_k(n+1) = \hat{b}_k(n) + \mu e(n)\hat{x}_b(n-k), \tag{22}$$
$$k = 0, 1, \ldots, N-1,$$
$$c(n+1) = c(n) - \mu_c e(n)[\hat{a}_0(n)\hat{x}_a(n-1) + \hat{b}_0(n)\hat{x}_b(n-1)], \tag{23}$$

and filtered-X reference signals $\hat{x}_a(n)$ and $\hat{x}_b(n)$ are calculated as a similar expression given in equation (12).

2.4 using recursive FLANN

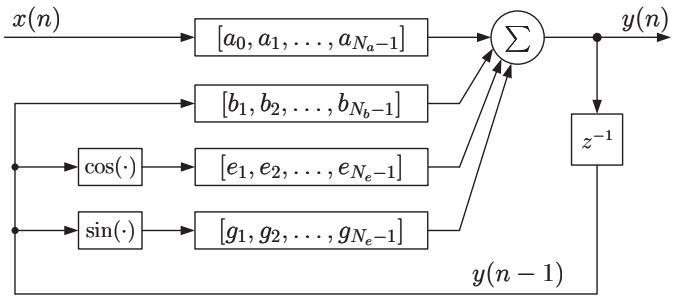

Figure 4 – Implementation of a recursive FLANN filter of order $P = 1$.

Recursive FLANN is another effective structure applied to nonlinear ANC system and the implementation of a recursive FLANN filter of order $P = 1$ is given in Figure 4 (22, 24). Using the recursive FLANN diagram block into ANC system shown in Figure 1, one has the secondary source $y(n)$ as follows:

$$y(n) = \sum_{i=0}^{N_a-1} a_i x(n-i) + \sum_{j=1}^{N_b-1} b_j y(n-j) + \sum_{k=0}^{N_e-1} e_k \cos[\pi y(n-k)] + \sum_{k=0}^{N_e-1} g_k \sin[\pi y(n-k)]. \tag{24}$$

Where, it has zero initial values, i.e. $y(-1) = \cdots = y(-N_y+1) = 0$ and $N_y = max(N_b, N_e)$. Following a similar way, we can derive the FXLMS algorithm for updating control filter weights and LMS algorithm for adjusting AR model coefficient respectively as

$$a_i(n+1) = a_i(n) + \mu e(n)\hat{x}(n-i),\ i = 0, 1, \ldots, N_a - 1, \tag{25}$$
$$b_j(n+1) = b_j(n) + \mu e(n)\hat{y}(n-j),\ j = 1, 2, \ldots, N_b - 1, \tag{26}$$
$$e_k(n+1) = e_k(n) + \mu e(n)\hat{y}_{\cos}(n-k),\ k = 1, 2, \ldots, N_e - 1, \tag{27}$$
$$g_k(n+1) = g_k(n) + \mu e(n)\hat{y}_{\sin}(n-k),\ k = 1, 2, \ldots, N_e - 1, \tag{28}$$
$$c(n+1) = c(n) - \mu_c e(n) a_0(n)\hat{x}(n-1), \tag{29}$$

where

$$\hat{y}(n) = \sum_{m=0}^{\hat{M}-1} \hat{s}_m y(n-m),$$
$$\hat{y}_{\cos}(n) = \sum_{m=0}^{\hat{M}-1} \hat{s}_m \cos[\pi y(n-m)],$$
$$\hat{y}_{\sin}(n) = \sum_{m=0}^{\hat{M}-1} \hat{s}_m \sin[\pi y(n-m)].$$

3. SIMULATIONS

Extensive simulations have been conducted for many scenarios to illustrate the effectiveness of the designed nonlinear NANC system with AR model in mitigating FM. The common conditions for simulations are given in Table 1. In addition, the FIR-type secondary path cutoff frequency is set to be 0.4π and it is identified by offline adaptive LMS algorithm. We performed 40 independent runs in all simulations to do the ensemble average.

Table 1 – Common conditions for simulations.

Parameters	Values
ω_p	0.1π
a_p, b_p	3.0, 1.0
a, b	1.0, 1.0
σ_p^2	0.01 (-20 dB)
$M, \hat{M}$	12, 12

Table 2 – Proper conditions and results for different simulation scenarios.

Filter type	% FM	Parameters and their values	Steady-state MSE	Weights number
Volterra filter	1%	$P=3, L_{\mathrm{V}}=8, \mu=0.0001, \mu_c=0.00005$	0.0102	84
	5%	$P=3, L_{\mathrm{V}}=12, \mu=0.0001, \mu_c=0.00005$	0.0114	286
	10%	$P=3, L_{\mathrm{V}}=12, \mu=0.0001, \mu_c=0.00005$	0.0114	286
FLANN	1%	$N=3, \mu=0.001, \mu_c=0.00025$	0.0106	6
	5%	$N=3, \mu=0.001, \mu_c=0.00025$	0.0106	6
	10%	$N=3, \mu=0.001, \mu_c=0.00025$	0.0106	6
	15%	$N=3, \mu=0.001, \mu_c=0.00025$	0.0106	6
	20%	$N=5, \mu=0.001, \mu_c=0.00025$	0.0108	10
	25%	$N=5, \mu=0.001, \mu_c=0.00025$	0.0108	10
Recursive FLANN	1%	$N_a=N_b=8, N_e=4, \mu=0.001, \mu_c=0.0005$	0.0145	21
	5%	$N_a=N_b=8, N_e=4, \mu=0.0005, \mu_c=0.0005$	0.0148	21
	10%	$N_a=N_b=24, N_e=12, \mu=0.00025, \mu_c=0.00025$	0.0158	71

In our simulations, different FM degrees noted by % FM ($:= |\Delta\omega|/\omega_p \times 100\,\%$) are investigated and the results are shown in Table 2 and Figures 5 to 7. Steady-state residual noise powers (MSEs) and control filter weights number contained in the system can be picked up to qualitatively describe performances of different nonlinear filters in accommodating FM.

As shown in Table 2 and Figure 5, it is clear that the order and length of Volterra filter should be increased to mitigate increasing FM. However, the number of filter weights will increase in geometric growth and the algorithm will converge slower. In fact, when we try to mitigate more than 10 % FM and we set order $P=3$ and length $L_{\mathrm{V}}=24$, this setup will lead to 2300 weights which needs enormous computation time to finish even one simulation run while without any effect. Meanwhile, Table 2 and Figure 7 tell us that recursive FLANN presents a relatively better performance as being applied to accommodating FM, since it converges faster and contains less weights. However, it is found that recursive FLANN will still suffer distinct performance degradation as trying to be used for mitigating more than 10 % FM. Finally, still from Table 2 and Figure 6, obviously, FLANN presents the most promising performance in accommodating FM during these three nonlinear methods and it could handle more than 25 % FM with much less weights and fast convergence.

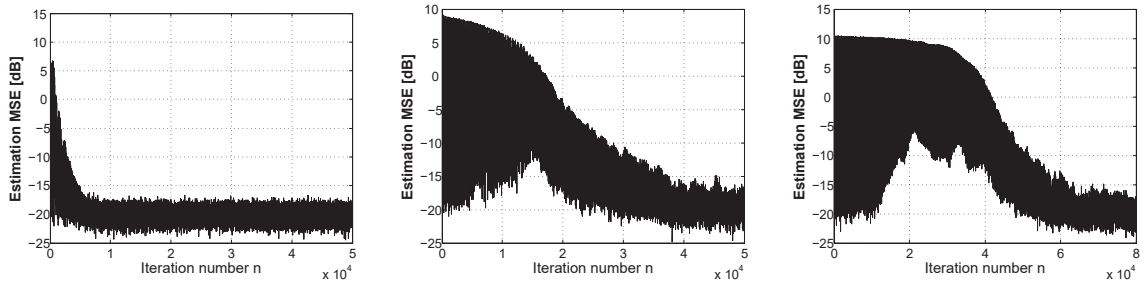

(a) (b) (c)

Figure 5 – Simulated MSE of nonlinear NANC system with Volterra filter when it is used for accommodating different FM degrees. (a) 1 % FM. (b) 5 % FM. (c) 10 % FM.

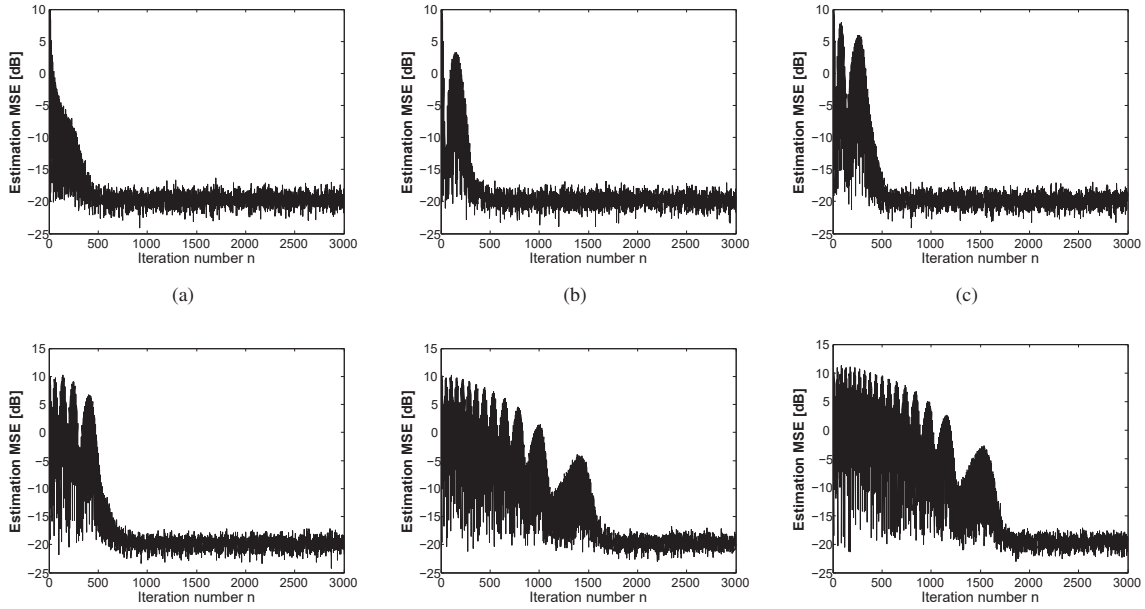

(a) (b) (c)

(d) (e) (f)

Figure 6 – Simulated MSE of nonlinear NANC system with FLANN when it is used for accommodating different FM degrees. (a) 1 % FM. (b) 5 % FM. (c) 10 % FM. (d) 15 % FM. (e) 20 % FM. (f) 25 % FM.

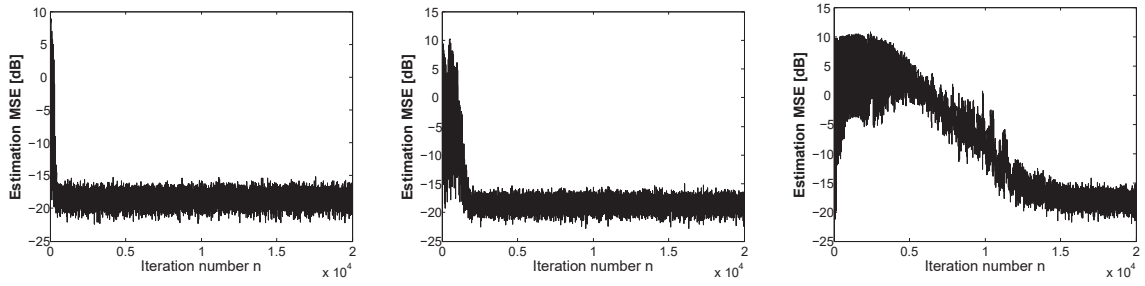

(a) (b) (c)

Figure 7 – Simulated MSE of nonlinear NANC system with recursive FLANN when it is used for accommodating different FM degrees. (a) 1 % FM. (b) 5 % FM. (c) 10 % FM.

4. CONCLUSIONS

In this paper, nonlinear NANC systems using Volterra filter, FLANN, and recursive FLANN coupling with AR model are designed for accommodating FM. Effectiveness of the new systems in mitigating FM have been verified through extensive simulations. Through detail performance comparisons, it is proved that FLANN filter is the most promising approach during them in suppressing narrowband noise in the presence of FM.

Topics for further research include a) extension of the proposed structure to multi-frequency case; b) new algorithms for FLANN, etc.

ACKNOWLEDGMENT

This work was supported in part by the National Natural Science Foundations of China (61201364) and the Fundamental Research Funds for the Central Universities (NS2016034).

REFERENCES

1. Elliott SJ, Nelson PA. Active noise control. IEEE Signal Processing Mag.. 1993; 10(4): 12–35.
2. Nelson PA, Elliott SJ. Active Control of Sound, 3rd ed. New York: Academic. 1995.
3. Kuo SM, Morgan DR. Active Noise Control Systems, Algorithms and DSP Implementations. New York: Wiley. 1996.
4. Elliott SJ. Signal Processing for Active Control. New York: Academic. 2001.
5. Chaplin GWB. The cancellation of repetitive noise and vibration. Proc. Inter-Noise. 1980: 699–702.
6. Morgan DR. An analysis of multiple correlation cancellation loops with a filter in the auxiliary path. IEEE Trans. Acoust., Speech, Signal Processing. 1980; ASSP-28(4): 454-467.
7. Burgess JC. Active adaptive sound control in a duct: A computer simulation. J. Acoust. Soc. Amer.. 1981; 70(3): 715–726.
8. Xiao Y, Ma L, Khorasani K. A robust narrowband active noise control system for accommodating frequency mismatch. Proc. of European Signal Processing Conf.. 2004: 917–920.
9. Xiao Y, Ikuta A, Ma L, Xu L, Ward RK. Statistical properties of the LMS Fourier Analyzer in the presence of frequency mismatch. IEEE Trans. Circuits Syst. I. 2004; 51(12): 2504–2515.
10. Sakai H, Hinamoto Y. An exact analysis of the LMS algorithm with tonal reference signals in the presence of frequency mismatch. Signal Processing. 2005; 85(6): 1255–1262.
11. Xiao Y, Ma L, Khorasani K, Ikuta A, Xu L. A filtered-X RLS based narrowband active noise control system in the presence of frequency mismatch. IEEE Int. Symp. On Circuits and Systems. 2005; 1: 260-263.
12. Xiao Y, Ma L, Khorasani K, Ikuta A. A new robust narrowband active noise control system in the presence of frequency mismatch. IEEE Trans. Audio, Speech, and Language Processing. 2006; 14(6): 2189–2200.
13. Hinamoto Y, Sakai H. A filtered-X LMS algorithm for sinusoidal reference signals—effects of frequency mismatch. IEEE signal processing letters. 2007; 14(4): 259–262.
14. Xiao Y, Ikuta A, Ma L, Khorasani K. Stochastic analysis of the FXLMS-based narrowband active noise control system. IEEE Trans. Audio, Speech, and Language Processing. 2008; 16(5): 1000–1014.
15. Jeon HJ, Chang TG, Kuo SM. Analysis of frequency mismatch in narrowband active noise control. IEEE Trans. Audio, Speech, and Language Processing. 2010; 18(6): 1632–1642.
16. Jeon HJ, Chang TG, Yu S, Kuo SM. A narrowband active noise control system with frequency corrector. IEEE Trans. Audio, Speech, and Language Processing. 2011; 19(4): 990–1002.
17. Liu J, Sun J, Xiao Y. Mean-sense behavior of filtered-X LMS algorithm in the presence of frequency mismatch. Proceedings of IEEE International Symposium on Intelligent Signal Processing and Communication Systems. 2012: 374–379.
18. Strauch P, Mulgrew B. Active control of nonlinear noise processes in a linear duct. IEEE Trans. Signal Processing. 1998; 46(9): 2404–2412.
19. Snyder SD, Tanaka N. Active control of vibration using a neural network. IEEE Trans. Neural Networks. 1995; 6(4): 819–828.

20. Bouchard M, Pailard B, Dinh CTL. Improved training of neural networks for non-linear active control of sound and vibration. IEEE Trans. Neural Networks. 1999; 10(2): 391–401.

21. Yu Z, Liu J, Liu D, Sun J. Adaptive ANFIS-based filter for active control of sinusoidal primary noise in nonlinear path. Journal of Harbin Institute of Technology (New series). 2011; 18(5): 137–142.

22. Das DP, Panda G. Active mitigation of nonlinear noise processes using a novel filtered-s LMS algorithm. IEEE Trans. Speech Audio Processing. 2004; 12(3): 313–322.

23. Sicuranza GL, Carini A. A generalized FLANN filter for nonlinear active noise control. IEEE Transactions on Audio, Speech, and Language Processing. 2011; 19(8):2412–2417.

24. Sicuranza GL, Carini A. Adaptive recursive FLANN for nonlinear active noise control. Proceedings of IEEE International Conference on Acoustics, Speech and Signal Processing. 2011; 125(3): 4312–4315.

25. Carini A, Sicuranza GL. A new class of FLANN filters with applications to nonlinear active noise control. Proc. of European Signal Processing Conf.. 2012: 1950–1954.

26. Behera SK, Das DP, Subudhi B. Functional link artificial nerual network applied to active noise control of a mixture of tonal and chaotic noise. Applied Soft Computing. 2014; 23: 51–60.

27. Kukde R, Manikandan MS, Panda G. Development of a nover narrowband active noise controller in presense of sensor error. Proceedings of International Conference on Advances in Computing, Communications and Informatics. 2014: 2735–2739.

28. Tan L, Jiang J. Filtered-X second-order Volterra adaptive algorithms. Electron. Lett.. 1997; 33(8): 671–672.

29. Tan L, Jiang J. Adaptive Volterra Filters for Active Control of Nonlinear Noise Processes. IEEE Transactions On Signal Processing. 2001; 49(8): 1667–1676.

30. Tan L, Jiang J. Adaptive Second-Order Volterra Filtered-X RLS Algorithms with Sequential and Partial Updates for Nonlinear Active Noise Control. Proceedings of 4th IEEE Conference on Industrial Electronics and Applications. 2009.

31. Liu J, Jing Q, Xiao Y. Nonlinear narrowband active noise control using Volterra filter. Proceedings of 21th International Congress of Sound and Vibration. 2014.

32. Raz GV, Veen BV. Baseband Volterra filters for implementing carrier based nonlinearities. IEEE Trans. Signal Processing. 1998; 46(1): 103–114.